THE USE OF GEOPHYSICAL MODELS FOR NUCLEAR EXPLOSION MONITORING

Michael E. Pasyanos, William R. Walter, Megan Flanagan, Rengin Gok, and Gregory A. Franz

Lawrence Livermore National Laboratory

Sponsored by National Nuclear Security Administration
Office of Nonproliferation Research and Development
Office of Defense Nuclear Nonproliferation

Contract No. W-7405-ENG-48

ABSTRACT

Geophysical models constitute an important component of calibration for nuclear explosion monitoring. Models take a wide variety of forms and scales and are used in a number of ways. We will focus on several of them here. The first that we discuss are regional tomography models. They can be constructed as 2-D, 2 1/2 D, or 3-D, depending on how the crust and upper mantle are parameterized, each having certain advantages (speed, accuracy, etc.). In any form, these are used to predict regional travel times such as Pn and Sn. The times derived by the models can be used as corrections to our arrival times, or simply as a background model for empirical measurements. We are also developing a number of fully 3-D models, including a priori geophysical models and stochastic models. The a priori WENA (Western Eurasia North Africa) model is a large-scale model that has been shown to compare favorably against a number of data sets and has been recently demonstrated to improve both travel-time and location estimates. We have also been using the Markov Chain Monte Carlo (MCMC) technique to produce stochastic models in the Yellow Sea–Korean Peninsula (YSKP) region. We are continuing to make improvements to this model by going to higher resolution and by incorporating more data sets to further narrow the range of acceptable models.

We maintain our efforts to develop models of surface wave dispersion and attenuation, and apply the results. Ambient noise tomography is being employed to further improve the resolution of the group velocities in certain regions as presented by Ritzwoller et al. (2006, these Proceedings). The maps are being used to isolate the fundamental mode surface wave and ensure that the signal passes dispersion and backazimuth tests when making Ms measurements, as presented by Bonner et al. (2006, these Proceedings). Attenuation models can be used to make corrections to surface wave amplitudes to account for regional amplitude variations that are important at shorter periods. We have been testing model-based attenuation models, as well as investigating the correlations between dispersion and attenuation. Surface wave group velocities can be inverted either alone, or in conjunction with other data, to derive models of the crust and upper mantle structure. We are using receiver functions, in joint inversions with the surface waves, to produce profiles directly under seismic stations throughout the region. By assembling the results from many stations, we can see how regional seismic phases are affected by complicated upper mantle structure, including lithospheric thickness and anisotropy. We will be showing the latest results from a study using data from the Eastern Turkey Seismic Experiment (ETSE) deployment. The joint inversion is used to map the boundary of the lithospheric hole in eastern Turkey where the phase Sn is blocked.

OBJECTIVE

Geophysical models constitute an important component of calibration for nuclear explosion monitoring. Models take a wide variety of forms and scales and are used in a number of ways. We will focus on several of them that have been developed at Lawrence Livermore National Laboratory (LLNL). Regional tomography models, such as those for upper mantle head-waves Pn and Sn, can be used to predict regional travel times. We are also developing a number of fully 3-D models, including a priori geophysical models and stochastic models. Stochastic models are data-driven models generated using an MCMC technique. This method combines a priori information with geophysical data from multiple sources (and varying sensitivities) to produce models that are most consistent with the constraints. We next consider surface wave models of velocity and attenuation. The dispersion models can be used to construct phase-matched filters, which can improve weak surface wave signal and calculate regionally determined M_S. Attenuation models can be used to further correct the surface wave amplitudes. Dispersion models can be used either alone or in conjunction with other data, such as receiver functions, to construct 3-D velocity models of the lithosphere. This method is a reliable way of obtaining the local velocity structure near a station from teleseismic events.

RESEARCH ACCOMPLISHED

Regional Tomography Models

Regional tomography models can be used to predict the travel times of regional phases such as Pn and Sn. While details of the various methodologies vary, they all generally tomographically distribute the slowness along the upper mantle leg of the path, while either inverting or making some sort of correction for the crustal legs. The advantages of such a method is that the tomography can be used to help estimate travel times of these regional phases, even when no direct measurements have been made at a particular station. Due to the propagation path of these phases, however, the spatial coverage is generally limited to a relatively narrow swath around seismic areas within about 1500 km from events, making it of limited use in aseismic regions. Another potential problem is that normalization in the tomography can dampen the full amplitude of the velocity anomalies.

Still, the utility of tomography is evident. Figure 1 shows P-wave velocities in the upper mantle determined from tomographic inversion. Paths were limited to ground truth (GT) events (Bondar et al., 2004), but still resulted in about 90,000 observations. The path map shows excellent coverage of western and central Europe, the Middle East, central Asia and south Asia. Coverage is poor in the ocean, North Africa, and Russia. The model shows fast velocities beneath oceans and old crust (India, the Russian Platform) and slow velocities beneath Red Sea, East African Rift, and the Tethys Belt. These models can be used to predict the travel time of these regional phases.

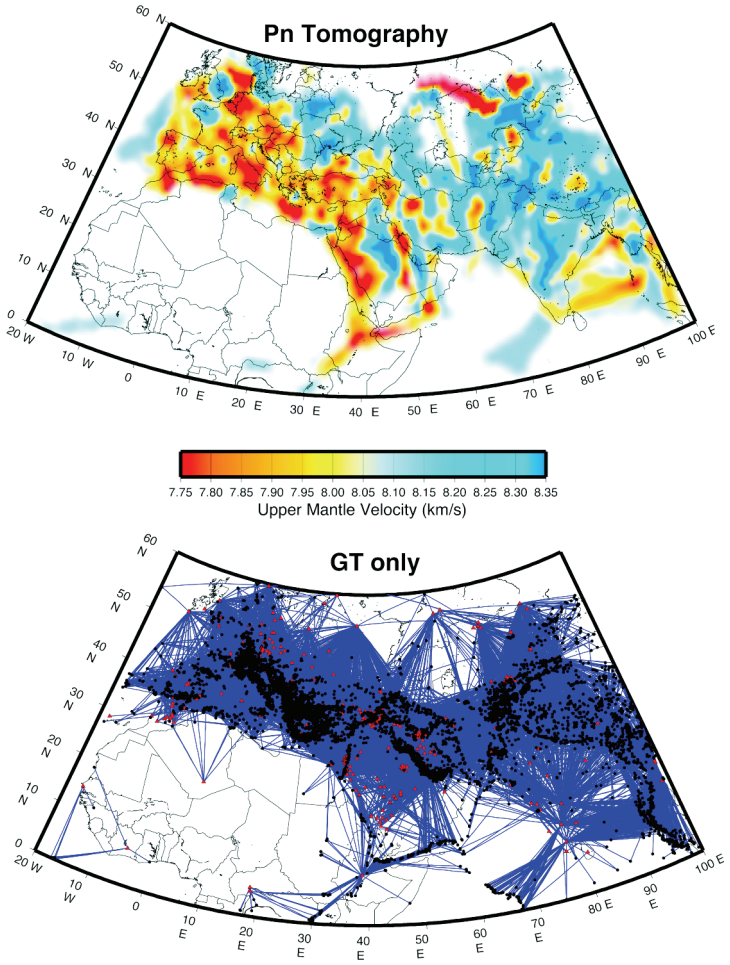

Figure 1. Uppermost mantle P-wave velocities derived from tomographic inversion (a) upper mantle velocities at 1º resolution and (b) the corresponding path map (Pasyanos et al., 2004).

A Priori Models

The WENA model is an a priori 3-D model for western Eurasia and North Africa (Pasyanos et al., 2004). Models like WENA can serve as background values for travel time correction surfaces and other derived parameters. We have demonstrated our ability to improve regional travel-time prediction and seismic event location accuracy using this model (Flanagan et al., 2006). Travel-time residuals are assessed relative to the IASPEI91 model (Kennett et al., 1995) for approximately 6,000 Pg, Pn, and P arrivals, from seismic events having 2σ epicenter accuracy between 1 km and 25 km (GT1 and GT25, respectively), recorded at 39 stations throughout the model region. Ray paths range in length between 0° and 40° (local, regional, and near teleseismic) providing depth sounding that spans the crust and upper mantle. The dataset also provides representative geographic sampling across Eurasia and North Africa including aseismic areas.

The WENA1.0 model markedly improves travel-time predictions for most stations with an average variance reduction of 29% for all ray paths from the GT25 events; when we consider GT5 and better events alone the variance reduction is 49%. For location tests we use 196 geographically distributed GT5 and better events. In 134 cases (68% of the events), locations are improved, and average mislocation is reduced from 24.9 km to 17.7 km. We develop a travel time uncertainty model (Figure 2) that is used to calculate location coverage ellipses. The coverage ellipses for WENA1.0 are validated to be representative of epicenter error and are smaller than those for IASPEI91 by 37%.

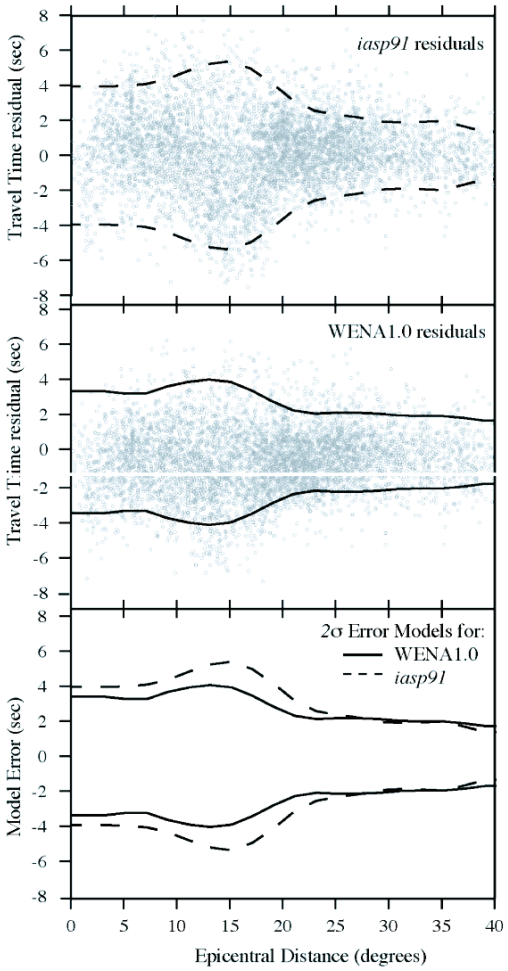

Figure 2. Distance-dependent uncertainty models for the IASPEI91 (top) and WENA1.0 (middle) velocity models. Note the nonstationarity and correlation in the travel-time uncertainty between 10° and 23° epicentral distance; uncertainty increases and errors are correlated (Flanagan et al., 2006).

In Figure 3, we find that the IASPEI91 variogram is non-stationary (levels off at the sill then increases again). The non stationarity is caused by long-period features in the travel time residual structure. WENA1.0 improves prediction of long-period residual features, and the variogram is relatively flat after the sill is reached. In some cases the sill value in the WENA1.0 variogram is reduced overall relative to the IASPEI91 variogram (e.g., station NUR), indicating that the 3-D model reduces the background variance. We conclude that a priori models are directly applicable where data coverage limits tomographic and empirical approaches, and the development of the uncertainty model enables merging of a priori and data-driven approaches using Bayesian techniques.

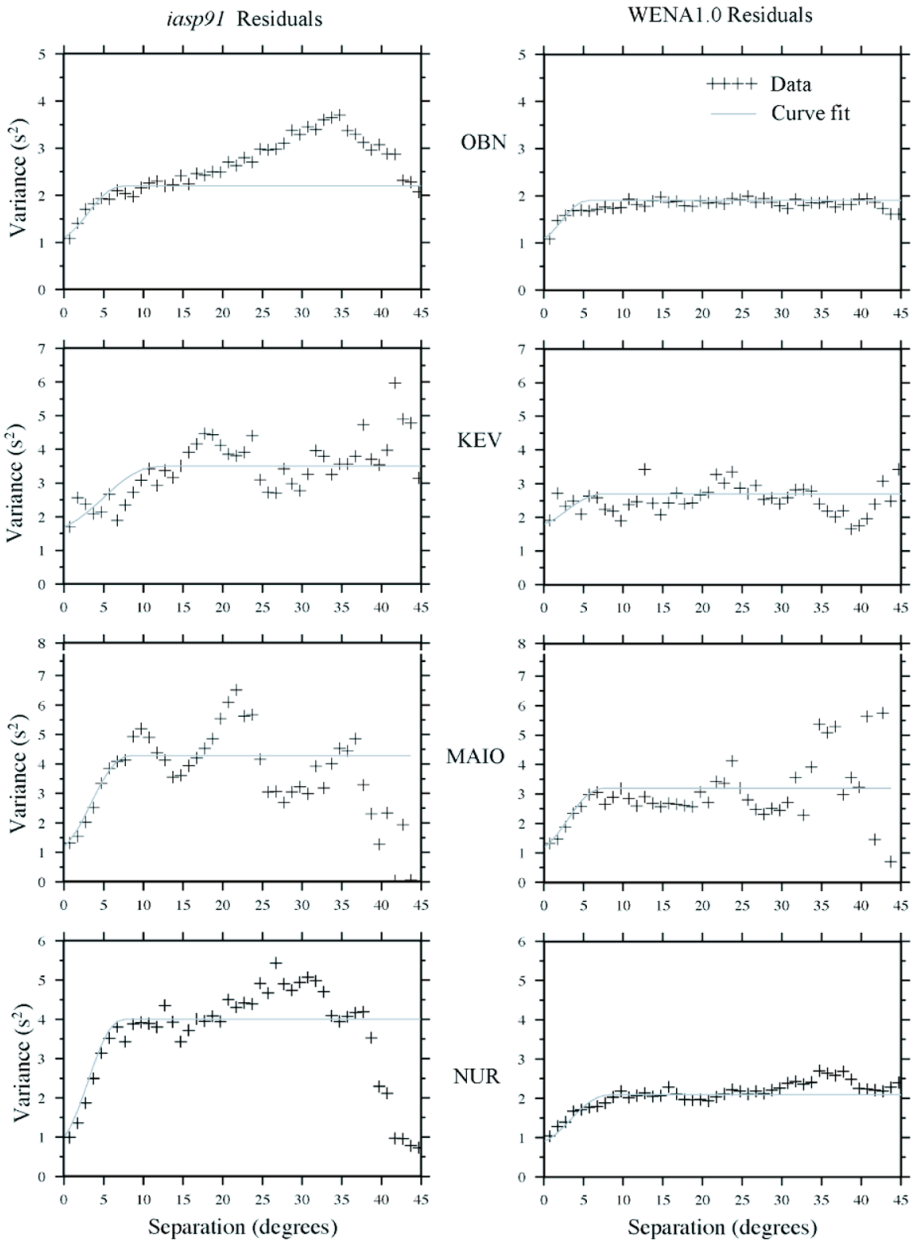

Figure 3. Variograms of travel time residuals at stations OBN, KEV, MAIO, and NUR for both the WENA1.0 and IASPEI91 velocity models. Crosses are the data variogram values in 1.0 degree bins; solid lines are the model variograms determined by curve fitting (Flanagan et al., 2006).

Stochastic Geophysical Models

We have been using the MCMC method to generate 3-D, data-driven stochastic models. We use MCMC to sample models from a prior distribution, test them against multiple data types in a staged approach, and develop a posterior distribution of seismic models that are most consistent with multiple seismic data sets (Pasyanos et al., 2006). This approach has several advantages over a single deterministic model. First, we are able to easily incorporate prior information on the model, such as the a priori geophysical models that were discussed earlier. Secondly, with this technique, we are able to reconcile different data types that can be used to constrain the model. We can also estimate the uncertainties of model parameters, properly migrating data uncertainties into model uncertainties. The method

does not constrain models to be normally distributed, but instead allows non-Gaussian or multi-modal distributions. Finally, we can estimate uncertainties on predicted observable signals, such as would be required to apply this model as a correction surface.

We use this method to determine the crust and upper mantle structure of the YSKP region using surface wave dispersion data, body wave travel time data, gravity, and receiver functions (Pasyanos et al., 2006). Figure 4 shows a crustal thickness map and corresponding uncertainties, taken by calculating the mean and standard deviation of the posterior distribution. One can see the thinning associated with the oceanic crust of the Pacific Ocean and Sea of Japan. We also use this model to predict waveforms using a spectral element model (Komatitsch et al., 2002; Rodgers et al., 2006, these Proceedings).

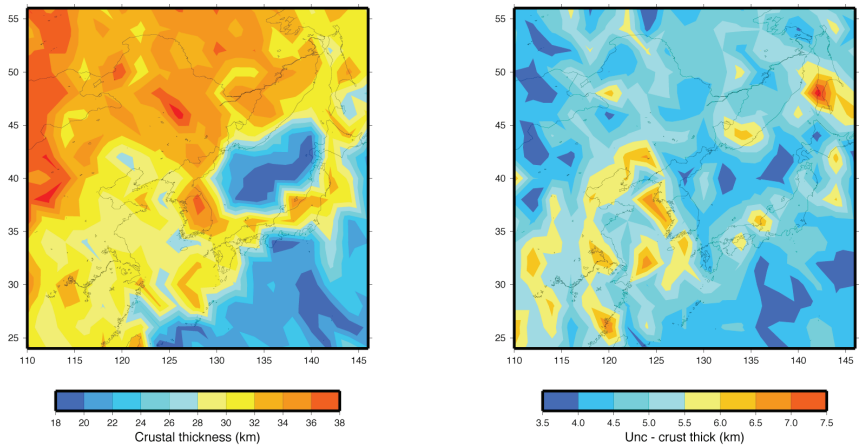

Figure 4. A crustal thickness map of the YSKP region determined using stochastic inversion methods, along with its associated uncertainties (Pasyanos et al., 2006).

Surface Wave Models

Over the past several years, LLNL has been developing surface wave models in Eurasia for nuclear explosion monitoring (Pasyanos et al., 2001; Pasyanos, 2005). Dispersion measurements are made using multiple narrow-band filters on deconvolved displacement data from the LLNL Seismic Research Knowledge Base (SRKB). We continue to improve upon our surface wave model by adding more paths, generally by taking advantage of new datasets, but also by revisiting stations with more recent events. Most recently, we have added measurements from stations in the Mediterranean (e.g., MIDSEA, Libya), India as presented by Bonner et al. (2006, these Proceedings), southern and central Africa, Alaska, and Siberia, including several PASSCAL deployments. To date, over 100,000 seismograms have been analyzed to determine the individual group velocities of 7–150 s Rayleigh and Love waves. Overall, we have made good quality dispersion measurements for 30,000 Rayleigh and 20,000 Love wave paths. Using a conjugate gradient method, we then tomographically invert these measurements to produce group velocity maps for Love and Rayleigh waves.

The group velocity models continue to improve in several ways. First, with more measurements, we have been able to expand the region of coverage to all of Eurasia and into Africa. By increasing the density of coverage in existing regions, we have increased the resolution of our model. Finally, we have been able to provide more reliable maps at short periods, expanding the frequency coverage down to 7 s period. We are able to resolve structural features associated with the tectonics of the region (Pasyanos, 2005). Path coverage will be further improved in the future by the use of cross-correlation of ambient seismic noise to derive the Green function between two stations, and from which the dispersion characteristics can be derived, as presented by Ritzwoller et al. (2006, these Proceedings). The benefits of this method in seismology have been dramatically demonstrated for southern California in Shapiro et al. (2005).

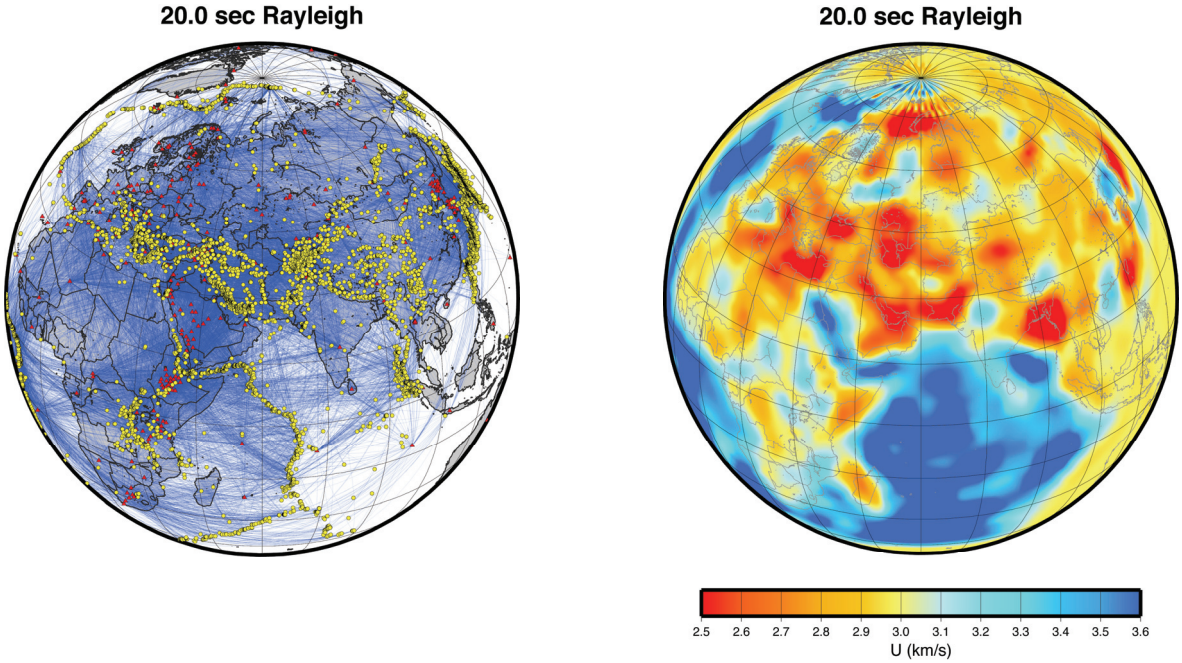

Figure 5. Surface wave dispersion maps for 20 s Rayleigh waves. (a) Path map showing coverage of the Eurasian and African continents. (b) Group velocity map of the same region (Pasyanos, 2005).

One application of surface wave models is to invert the results to derive models of the crust and upper mantle structure. This is particularly useful in aseismic regions that are poorly sampled by other datasets. By combining the surface wave data with other data, we can reduce the non-uniqueness inherent in the profile inversions performed using only surface wave data. In the next section, for example, we will be using the surface wave data in combination with teleseismic receiver functions.

Another application of the group velocities is to construct phase-matched filters in combination with regional surface-wave magnitude formulas to improve the mb:Ms discriminant and extend it to smaller magnitude events. Phase matched filtering has been shown to effectively winnow out any unwanted signals from the surface wave signal. Regional surface wave magnitudes calculated using narrow-band filters (Russell, 2006) from the cleaned signal show a more consistent magnitude value between periods, as presented by Bonner et al. (2006, these Proceedings).

Ms magnitudes can be further improved by making corrections based on surface wave attenuation maps.
One approach is to calculate model-based attenuation values from geophysical models, such as the WENA model (Pasyanos et al., 2004). An example of such a map is shown in Figure 6 for 15 s Rayleigh waves. Attenuation is high (Q is low) where we find large sedimentary basins, either oceanic or continental. Low Q is found in regions with fast, competent upper crust and is particularly low in abyssal oceanic crust. These model-based maps could be tested and validated by comparing model-based predictions to empirical maps in regions where these have been developed.

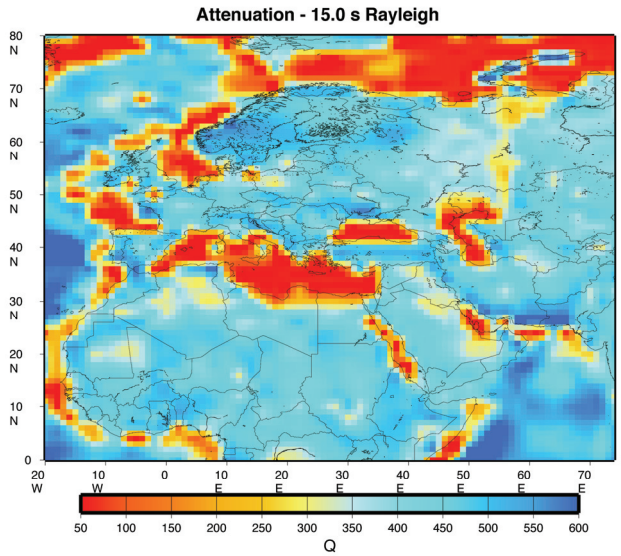

Figure 6. Map of the model-based surface wave attenuation parameter Q for 15 s Rayleigh waves.

Another approach would be to take both the attenuation and dispersion measurements and derive a relationship between the two. For example, we have correlated the group velocity tomography models to the surface wave attenuation model of Selby et al. (2001) to see if there are correlations between the two. Similar correlations could be made with other global models of surface wave attenuation (e.g. Dalton and Ekström, 2006) but currently only for long periods. We have also correlated the velocity model to the model-based attenuation maps. Figure 7 shows the correlation for 20 s where, although there is a lot of scatter, we can clearly see the trend between the two parameters (solid line). Here, we find that in regions with thick sediments that have both slow velocities and high attenuation, the group velocities are slow and the attenuation parameter $\gamma = \frac{\pi}{UQT}$ is high. In contrast, on the other end of the plot in oceanic crust, the velocities are high while the attenuation is low. Once such relationships have been established, then attenuation models can be easily constructed. One of the advantages of this technique is that the resolution would far-exceed the resolution available performing an attenuation tomography.

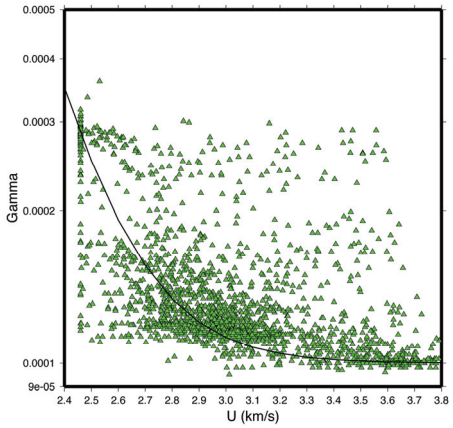

Figure 7. A comparison of tomographically-based group velocities and model-based attenuation parameters.

Receiver Function Profiles

We are also using receiver functions, in joint inversions with the surface waves, to produce profiles directly under seismic stations throughout the region. These two data types are complementary since receiver functions are sensitive to velocity contrasts, and surface waves are sensitive to depth-averaged velocity.

Here, we have applied this methodology to stations from the ETSE IRIS program that manages seismic equipment (PASSCAL) deployment (Gok et al., 2006). We jointly invert for the S-wave velocity structure, Moho depth and mantle-lid (lithospheric mantle) thickness. We also estimated the transverse anisotropy due to Love and Rayleigh wave propagation discrepancies.

We found anomalously low shear wave velocities underneath the Anatolian Plateau. Average crustal thickness is 36 km in the Arabian Plate, 44 km in Anatolian Block and 48 km in the Anatolian Plateau (Figure 8). We observe very low shear wave velocities at the crustal portion (30–38 km) of the northeastern part of the Anatolian Plateau. The lithospheric mantle thickness is either not thick enough to resolve it or it is completely removed underneath the Anatolian Plateau. The shear velocities and anisotropy down to 100 km depth suggest that the average lithosphere-asthenosphere boundary in the Arabian Plate is about 90 km and 70 km in Anatolian block. The study reveals three different lithospheric structures in eastern Turkey: Anatolian plateau (east of Karliova junction), Anatolian block and the northernmost portion of the Arabian plate. The boundaries of differences in lithospheric structure coincide with the major tectonic boundaries.

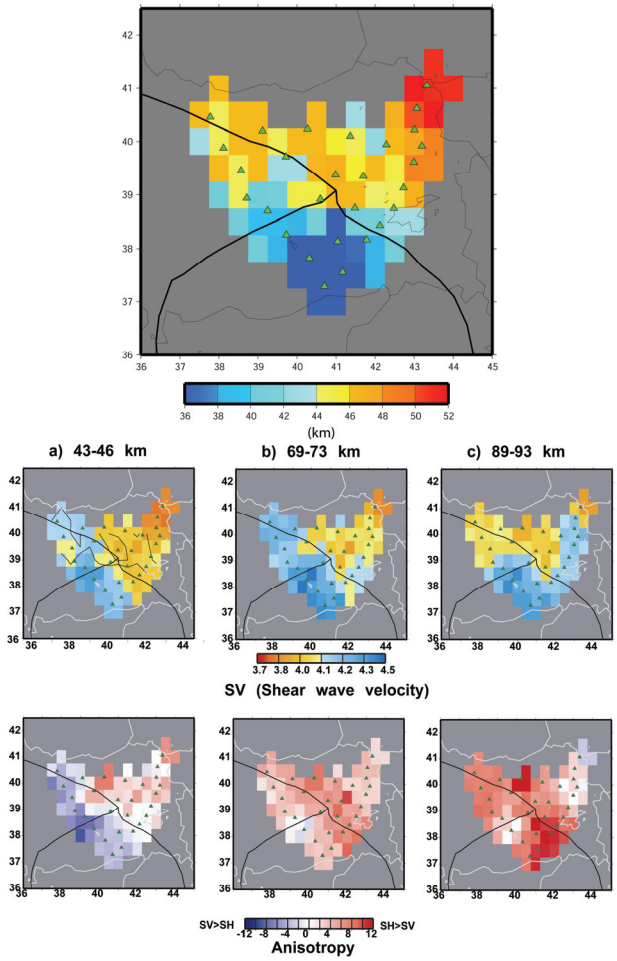

Figure 8. Results from the joint inversion of receiver functions and surface waves from ETSE stations in eastern Turkey. Upper figure: crustal thickness map. Lower figure: shear wave velocity and anisotropy for several mantle depth slices (Gok et al., 2006).

CONCLUSIONS AND RECOMMENDATIONS

Geophysical models are used in a variety of ways for nuclear explosion monitoring. We have presented a variety of models being developed at LLNL, often in coordination with other institutions, including regional tomography models, a priori models, stochastic models, surface wave models, and receiver function models. They can be used to calibrate and represent the calibration of structure under stations, predict travel times, assess phase behavior, and improve discrimination.

REFERENCES

Bondar, I., S. C. Myers, E. R. Engdahl, and E. A. Bergman (2004). Epicentre accuracy based on seismic network criteria, *Geophys. J. Int.* 156: 483–496.

Dalton, C. A. and G. Ekström (2006). Global models of surface wave attenuation, *J. Geophys. Res.* 111: B05317, doi:10.1029/2005JB003997.

Flanagan, M. P., S. C. Myers, and K. D. Koper (2006). Regional travel-time uncertainty and seismic location improvement using a 3-dimensional a priori velocity model, *Bull. Seism. Soc. Amer*. (submitted).

Gok, R., M. E. Pasyanos, and E. Zor (2006). Lithospheric structure of the continent-continent collision zone: Eastern Turkey, *J. Geophys. Res.* (submitted).

Kennett, B. L. N., E. R. Engdahl, and R. Buland (1995). Travel times for global earthquake location and phase association, *Geophys. J. Int*. 122: 108–124.

Komatitsch, D., J. Ritsema, J. Tromp (2002). The spectral-element method, Beowulf computing, and global seismology, *Science*, 298: 1,737–1,742.

Pasyanos, M. E., W. R. Walter, and S. E. Hazler (2001). A surface wave dispersion study of the Middle East and North Africa for monitoring the comprehensive nuclear-test-ban treaty, *Pure Appl. Geophys.* 158: 1,445–1,474.

Pasyanos, M. E., W. R. Walter, M. P. Flanagan, P. Goldstein, and J. Bhattacharyya (2004). Building and testing an a priori geophysical model for western Eurasia and North Africa, *Pure Appl. Geophys.* 161: 235–281.

Pasyanos, M. E. (2005). A variable-resolution surface wave dispersion study of Eurasia, North Africa, and surrounding regions, *J. Geophys. Res*. 110: B12301, doi:10.1029/2005JB003749.

Pasyanos, M. E., G. A. Franz, and A. L. Ramirez (2006). Reconciling data using Markov Chain Monte Carlo: An application to the Yellow Sea–Korean Peninsula region, *J. Geophys. Res*. 111: B03313, doi:10.1029/2005JB003851.

Russell, D. R. (2006). Development of a time-domain, variable-period surface wave magnitude measurement procedure for application at regional and teleseismic distances. Part I: Theory, *Bull. Seism. Soc. Amer.* 96: 665–677.

Selby, N. (2001). Association of Rayleigh waves using back azimuth measurements: Application to test ban verification, *Bull. Seism. Soc. Am.* 91: 580–593.

Shapiro, N. M., M. Campillo, L. Stehly, and M. H. Ritzwoller (2005). High resolution surface wave tomography from ambient seismic noise, *Science,* 307: 1,615–1,618.